Available online at www.sciencedirect.com
SCIENCE DIRECT®
Journal of Solid State Chemistry 177 (2004) 2150–2157
JOURNAL OF SOLID STATE CHEMISTRY
http://elsevier.com/locate/jssc

Temperature behavior of the protonic conductor $K_4LiH_3(SO_4)_4$

A. Haznar* and A. Pietraszko

Institute of Low Temperature and Structure Research, Polish Academy of Science, ul. Okólna 2, P.O. Box 1410, 50-950 Wrocław 2, Poland

Received 3 November 2003; received in revised form 22 December 2003; accepted 7 January 2004

Abstract

The results of the X-ray structural study for the $K_4LiH_3(SO_4)_4$ single crystal are presented at a wide temperature range. The thermal expansion of the crystal using the X-ray dilatometry and the capacitance dilatometry from 8 to 500 K was carried out. The crystal structures data collection, solution and refinement at 125, 295, 443 and 480 K were performed. The $K_4LiH_3(SO_4)_4$ crystal has tetragonal symmetry with the $P4_1$ space group ($Z = 4$) at room temperature as well as at the considered temperature range. The existence of a low-temperature, para–ferroelastic phase transition at about 120 K is excluded. The layered structure of the crystal reflects a cleavage plane parallel to (001) and an anisotropy of the protonic conductivity. The superionic high-temperature phase transition at $T_S = 425$ K is isostructural. Nevertheless, taking into account an increase of the SO_4 tetrahedra libration above T_S, a mechanism of the Grotthus type could be applied for the proton transport explanation.

Keywords: $K_4LiH_3(SO_4)_4$; Crystal structure; Phase transition; Thermal expansion; Protonic conductor; X-ray diffraction

1. Introduction

Some crystals of general formula $Me_4LiH_3(XO_4)_4$, where $Me = NH_4$, Rb, K and $X =$ Se, S (further abbreviated MeLHX), have been known for more than hundred years but their ferroelastic properties have only been reported since 1988 [1–4]. Interest in the crystal family has increased since the superionic phase was discovered [5–7].

Although a large majority of papers are focused on elastic properties of the crystals at low temperatures, existence of the ferroelastic phase in KLHS remains ambiguous. Anomalies connected with the appearance of the phase transition in the KLHS crystal at a temperature range 110–120 K were detected by an EPR study [4], IR spectroscopy [8] and elastic properties of the crystal measurements [9,10]. At the same time a lack of a domain structure [6,7,9] and absence of an anomaly on the temperature dependence of the thermal expansion of the crystal at the mentioned temperature range [7] testify against the transition.

Similarly, there are only preliminary results concerning superionic phase in these crystals. As it has already been reported [5,7], transition to the superionic state is connected with the lowering of the activation energy of the conductivity. But a mechanism of the proton transport has not been explained yet, and structural data have been restricted to the prototype and low-temperature phases of the RLHS crystal [11,12].

The results of the X-ray [6,11,13] and the neutron [12] crystal structure solution and refinement indicated a common room-temperature, tetragonal symmetry, with $P4_1$ or $P4_3$ space group and four molecules of the $Me_4LiH_3(XO_4)_4$ in the unit cell. The XO_4 tetrahedra with Me ions in between form sandwiches stacked along the c-axis, which are connected by Li ions. The other characteristic structure features are tetramers of XO_4 joined by hydrogen bonds of length $\sim$2.5 Å XO_4, which are turned 90° around the c-axis in the neighboring layers. The transition to the ferroelastic phase is associated with the crystal symmetry lowering to the $P2_1$ space group characterized by a monoclinic distortion in the (001) plane.

Contrary to the previous results, Mróz et al. [12], using high-resolution neutron powder diffraction studies, have suggested that KLHS (as the only one of its family) has a monoclinic symmetry at room temperature as well as at low temperatures.

Taking into account the uncertainties related to the symmetry and the phase transitions of the KLHS crystal, we report the results of detailed structural

*Corresponding author. Fax: +48-71-441-029.
E-mail address: haznar@int.pan.wroc.pl (A. Haznar).

0022-4596/$ - see front matter © 2004 Elsevier Inc. All rights reserved.
doi:10.1016/j.jssc.2004.01.014

investigations from 8 K to the temperature of the crystal melting (about 500 K) based on the X-ray single-crystal diffraction study and the X-ray and capacitance dilatometry.

2. Experiment

Colorless, transparent, good-quality monocrystals of tetragonal bipyramid shape were grown by evaporation of aqueous solution Li_2CO_3 and K_2CO_3 in the molar ratio 1:4 and amount of H_2SO_4 to settle pH < 1. The material was purified by 3-fold recrystallization with an excess of the acid [5,6].

KLHS seems to be the most suitable material of the $Me_4LiH_3(XO_4)_4$ crystals due to its good mechanical properties, which allow obtaining a spherical shape of a sample minimizing the absorption error, and distinct from the other crystals from its family, KLHS is not hygroscopic.

A crystal for the X-ray experiment was ground in a compressed-air mil to a sphere of 0.3 mm diameter. For the dilatometric experiment the crystal was cut perpendicular to the main crystallographic directions onto the cube sample of $5.75 \times 5.75 \times 5.07\,mm^3$.

Measurements of the thermal expansion of the bulk KLHS crystal were performed by capacitance dilatometry [14,15] at the temperature range 8–200 K and X-ray dilatometry (Bond method) at the temperature range 90–500 K.

The capacitance was measured using an ultra-precise (sensitivity of 10^{-7} pF) capacitance bridge (Andeen-Hagerling 2500A) and a frequency of 1 kHz. Temperature was controlled by ITC-503 Oxford Instruments device. The measurement precision $\Delta l/l$ was $\sim 10^{-8}$.

Temperature dependence of the KLHS crystal lattice parameters was determined by the Bond method [16] using seven reflections: (6 –6 15), (5 –8 1), (0 6 28), (6 0 28), (3 –8 15), (8 5 1), (8 3 15), with $\theta > 75°$. The measurements were performed with a four-circle Kuma KM-4 diffractometer designed for precise lattice parameter determination [17] by the reflection method. The accuracy $\Delta a/a$, estimated by the least square method, was better than 5×10^{-5}.

Single-crystal X-ray diffraction data for structure determination were measured with Kuma KM-4 diffractometer at temperatures of 125, 295, 443, 480 K. The crystal stability and orientation were monitored by checking the intensities of two standard reflections after every 50 reflections. Details of data collection and structure refinement at 295 K are given in Table 1. The crystal structure refinement for the tetragonal $P4_1$ space group at temperatures of 125, 443 and 480 K led to final discrepancy factors R 2.29%, 3.71% and 3.78%, respectively.

Table 1
Details of single-crystal X-ray data collection and structure refinement at 295 K

Crystal data:	
Crystal system	Tetragonal
Space group	$P4_1$
a (Å)	7.397
c (Å)	28.691
V (Å^3)	1569.85
Z	4
Density calc. (mg/m^3)	2.33
Absorption coeff. μ (mm^{-1})	15.89
Data collection:	
Radiation, wavelength (Å)	CuK_α, 1.54056
Monochromator	Graphite
2θ range (deg)	156.51
Scan type	$\omega/2\theta$
Index range	h: −9, 9
	k: −8, 3
	l: −36, 36
No. reflections collected	8639
No. independent reflections	3312
No. observed reflections	3101
Decay of standard reflections	Negligible
Refinement:	
Refinement on	F^2
F_0 criterion	$\|F_0\| \geqslant 2\sigma(F_0)$
Corrections	
Lorentz polarization	
Absorption	For sphere
Extinction (empirical as in SHELXL93)	0.0116(3)
R_{Int}	0.047
Number of varied parameters	238
Final R_1	0.0302
Final wR_2	0.0716
Goodness of fit	1.061
Min. and max. residual (eÅ^3)	−0.31, 0.62

During the Bond method experiment and structure data collection from 90 to 300 K temperature was controlled by a CPC511 Oxford Cryosystem device with nitrogen blow and at a temperature range of 300–500 K by the Kuma Diffraction device with blowing of hot air. In both cases, temperature was stabilized with an accuracy of $\pm 0.3°$.

Program SHELXL-97 [18] was used for structure solution and refinement, while interatomic distance correction calculations of atoms vibrations according to thermal parameters were performed using SHELXTL/PC program [19].

3. Results and discussion

The aim of our paper is to discuss the temperature behavior of the KLHS crystal from the very low temperatures to its melting point. We would like to address the following questions:

- What is the symmetry of the crystal at room temperature?
- Does the crystal undergo any low-temperature phase transitions?
- How does the crystal structure change during the high-temperature (superionic) phase transition?
- What is the mechanism of the proton transport in the crystal?

3.1. Phase transitions

Cell dimension change versus temperature indicate well a phase transition since transformation of a crystal to a new phase is most often accompanied by a symmetry change. Almost all crystals of the $Me_4LiH_3(XO_4)_4$ family undergo paraelastic–ferroelastic phase transition at low temperatures [2,7,20–23]. Such a transition is associated with the crystal symmetry lowering type 4F2 from the tetragonal $P4_1$ to the monoclinic $P2_1$ space group and a domain structure appearance [24–26]. In the X-ray diffraction experiment domain structure manifest itself as a reflection splitting. And as far as the thermal expansion of a crystal is a consequence of the crystal network anharmonic vibrations, the transition to the superionic state should also reflect on the lattice parameters temperature dependence, especially when proton transport is closely related to the dynamics of the nearest surrounding.

The results of the Bond method experiment at the temperature range of 90–500 K are presented in Fig. 1a and b and the results of the capacitance dilatometry measurements at the temperature range of 8–200 K are presented in Fig. 2a and b.

The precise lattice parameter measurements have shown that the KLHS crystal just like the other crystals from its family has a tetragonal symmetry at room temperature. The unit-cell parameters a and b are equal and γ does not vary from 90° at the whole temperature range, which suggests a tetragonal symmetry.

The thermal expansion measurements of the crystal made using two methods have not shown any anomalies, which could suggest transition to the other crystallographic system, both at 110–120 K and at about 425 K. Such an experimental result and a lack of a domain structure below 110 K are indications that there is no ferroelastic transformation in the KLHS crystal. And the superionic phase transition of the crystal seems to be an isostructural one.

The thermal expansion coefficients of the KLHS crystal, α, have a typical value for the solid state. It is worth pointing out that the α value along [100] direction is smaller than along [001]. It reflects a layered structure of the crystal, where the cleavage plane is parallel to (001).

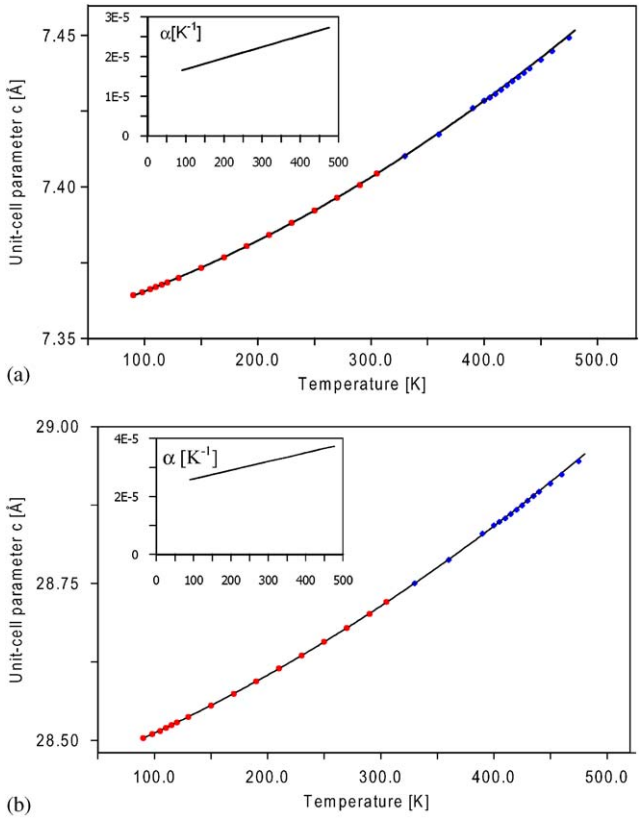

Fig. 1. Thermal expansion of the KLHS crystal measured by X-ray dilatometry (Bond method) at the temperature range of 90–500 K presented together with thermal expansion parameter in the insertion for the direction of: (a) a unit cell vector, and (b) c unit cell vector.

3.2. The crystal structure

Considering our research, we can admit that KLHS is isostructural with other compounds of the $Me_4LiH_3(XO_4)_4$ family [11,12]. The KLHS structure solution and refinement at temperatures of 125, 295 K and above the transformation to the superionic state at 443, 480 K confirmed that the crystal has tetragonal symmetry $P4_1$ ($Z = 4$) and the high-temperature phase transition takes place without symmetry change.

Details of the data collection and refinement at 295 K are given in Table 1, atomic coordinates and equivalent isotropic displacements are presented in Table 2 and selected bond lengths in Table 3. Flack parameter values close to zero (0.0085 at room temperature) indicate absence of an enantiomorphic phase contrary to Zúñiga et al. [11]'s suggestion for the $Rb_4LiH_3(SO_4)_4$ crystal.

The SO_4 tetrahedra with K ions in between form four sandwiches stacked along the c-tetragonal axis in the KLHS unit cell (Fig. 3). Each of the independent K ions is surrounded by eight sulfate O atoms at distances from 2.689 to 3.191 Å. The SO_4 tetrahedra are arranged in two layers in the sandwich and the characteristic deformation and distances between them suggest the

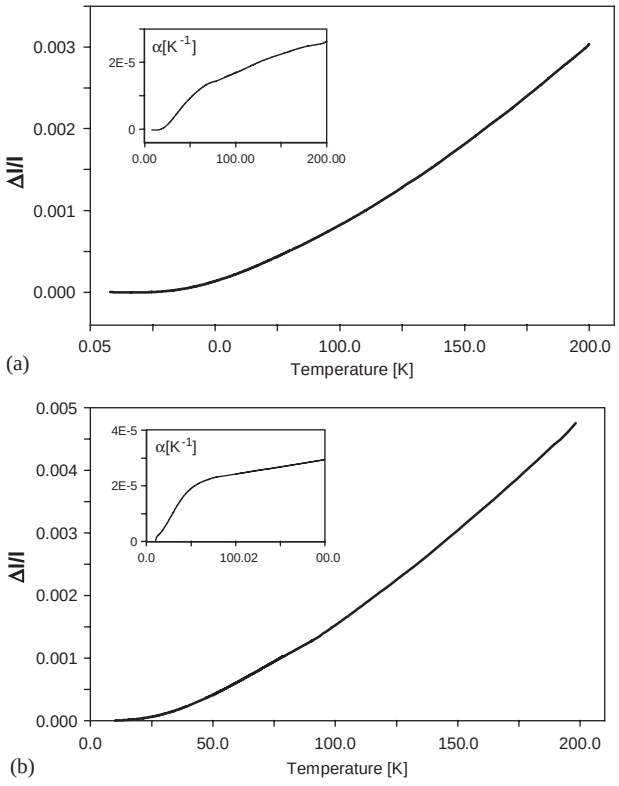

Fig. 2. Thermal expansion of the KLHS crystal measured by capacitance dilatometry at the temperature range of 8–200 K presented together with thermal expansion parameter in the insertion for the direction of: (a) *a* unit cell vector, and (b) *c* unit cell vector.

Table 2
Atomic positional parameters ($\times 10^4$) and thermal displacement amplitudes U_{iso} (Å^2) ($\times 10^3$) at 295 K

Atom	*x*	*y*	*z*	U_{iso}
K(1)	3757(1)	3992(1)	2565(1)	28(1)
K(2)	4936(1)	−2128(1)	1418(1)	24(1)
K(3)	10807(1)	−963(1)	2427	24(1)
K(4)	9851(1)	4898(1)	1316(1)	28(1)
S(1)	5477(1)	−1088(1)	2585	16(1)
S(2)	8917(1)	4286(1)	2589(1)	16(1)
S(3)	10089(1)	−207(1)	1256(1)	16(1)
S(4)	4728(1)	3227(1)	1298(1)	17(1)
O(11)	7023(4)	−677(4)	2290(1)	29(1)
O(12)	6253(4)	−1878(4)	3043(1)	28(1)
O(13)	4344(3)	−2444(3)	2372(1)	25(1)
O(14)	4466(4)	461(4)	2738(1)	31(1)
O(21)	7486(4)	3664(4)	2283(1)	36(1)
O(22)	8157(5)	5263(4)	2983(1)	41(1)
O(23)	9913(4)	2641(3)	2785(1)	28(1)
O(24)	10232(4)	5328(4)	2340(1)	35(1)
O(31)	9544(4)	1134(3)	1602(1)	26(1)
O(32)	8438(3)	−1145(4)	1065(1)	28(1)
O(33)	10995(4)	697(4)	864(1)	33(1)
O(34)	11225(4)	−1559(4)	1473(1)	28(1)
O(41)	5194(4)	1635(4)	1565(1)	32(1)
O(42)	3879(4)	2538(4)	835(1)	30(1)
O(43)	3407(4)	4325(4)	1535(1)	31(1)
O(44)	6276(4)	4257(4)	1142(1)	32(1)
Li	7342(8)	1491(7)	1931(2)	22(1)
H(1)	6915(81)	−3034(82)	2992(19)	44(14)
H(2)	2659(118)	2104(112)	858(28)	97(27)
H(3)	9403(123)	1965(133)	3107(29)	107(27)

existence of hydrogen bonds in the crystal. The sandwiches are connected by Li ions. Lithium ions are tetrahedrally coordinated and the average distance Li–O is about 1.9 Å. Distances K–O, Li–O and S–O in the KLHS crystal are comparable with those obtained for $KliSO_4$ [27] and $Rb_4LiH_3(SO_4)_4$ [11].

3.3. The hydrogen bonding

In the double layers called sandwiches, the SO_4 tetrahedra are joined by hydrogen bonds. Hydrogen bonds play an essential role in a proton transport in the solid state but up to now only preliminary studies of the hydrogen bonding type and its temperature changes in the $Me_4LiH_3(XO_4)_4$ crystals have been carried out [12,13].

As it was shown by Thomas and Liminga [30], only for short hydrogen bonds the proton influence on the donor and acceptor electron density is large enough to obtain proper information about hydrogen atom position from the X-ray experiment. Nevertheless, the character of hydrogen bonds can be detected indirectly (not only by the H atom position) due to differences between charge–density functions of the donor and acceptor groups, which manifest itself in their structural dimensions, as described by Katrusiak [28,29]. Also, the best chance for proton position estimation is in crystals consisting of light atoms, just like the KLHS crystal.

First of all, O···O distances are generally indicative of hydrogen bonding. There are only three distances between oxygen atoms of various tetrahedra in the KLHS structure of about 2.5 Å and the rest of them exceed 3 Å. The SO_4 tetrahedra, slightly deformed by the H bonds, form tetramers (Fig. 4). The tetramers are parallel to each other in a double layer but perpendicular to the tetramers in neighboring sandwiches. The hydrogen bond parameters at 295 and 480 K (above the superionic transition) are given in Table 4.

Slightly longer H1 and H2 bonds differ from the H3 bond (in the middle of the tetramer). The structural dimensions of the donor and the acceptor group [28,29] in the H1 and H2 bonds such as d(S1–O12) > d(S2–O22), d(S4–O42) > d(S3–O33), $\eta_d > \eta_a$, $\eta'_d > \eta'_a$ and proton positions suggest that these H bonds are ordered and asymmetrical.

The "dimers" of the SO_4 tetrahedra linked by H1 and H2 bonds are situated in parallel layers and are joined into sandwich by the short H3 bond. At room temperature, differences between donor and acceptor group of H3 bond are revealed as d(S2–O23) > d(S3–O32). But almost equal values of η'_d and η'_a suggest that the middle hydrogen bond is disordered with an

Table 3
Selected bond lengths (Å) at 295 K

K(1)–O(14)	2.709(3)
K(1)–O(13)^{iv}	2.729(3)
K(1)–O(42)^{v}	2.859(3)
K(1)–O(24)^{vi}	2.862(3)
K(1)–O(21)	2.886(3)
K(1)–O(43)	2.977(3)
K(1)–O(23)^{vi}	3.079(3)
K(1)–O(44)^{v}	3.116(3)
K(2)–O(22)^{viii}	2.697(3)
K(2)–O(13)	2.781(3)
K(2)–O(34)^{vi}	2.782(3)
K(2)–O(41)	2.821(3)
K(2)–O(32)	2.875(3)
K(2)–O(43)^{ii}	2.877(3)
K(2)–O(44)^{ii}	2.961(3)
K(2)–O(11)	3.128(3)
S(1)–O(14)	1.437(3)
S(1)–O(13)	1.443(2)
S(1)–O(11)	1.456(2)
S(1)–O(12)	1.547(3)
S(2)–O(24)	1.432(3)
S(2)–O(21)	1.450(3)
S(2)–O(22)	1.455(2)
S(2)–O(23)	1.530(2)
Li–O(11)	1.920(6)
Li–O(21)	1.901(7)
Li–O(31)	1.901(7)
Li–O(41)	1.908(7)
K(3)–O(33)^{i}	2.689(3)
K(3)–O(24)^{ii}	2.787(3)
K(3)–O(34)	2.791(3)
K(3)–O(11)	2.834(3)
K(3)–O(13)^{iii}	2.841(3)
K(3)–O(23)	2.933(3)
K(3)–O(31)	2.979(3)
K(3)–O(14)^{iii}	3.039(3)
K(4)–O(44)	2.733(3)
K(4)–O(43)^{iii}	2.738(3)
K(4)–O(34)^{iv}	2.846(3)
K(4)–O(12)^{vii}	2.860(3)
K(4)–O(31)	2.912(3)
K(4)–O(24)	2.967(3)
K(4)–O(14)^{vii}	3.118(3)
K(4)–O(32)^{iv}	3.191(3)
S(3)–O(34)	1.446(3)
S(3)–O(31)	1.460(3)
S(3)–O(33)	1.472(3)
S(3)–O(32)	1.508(2)
S(4)–O(43)	1.441(3)
S(4)–O(41)	1.446(3)
S(4)–O(44)	1.446(3)
S(4)–O(42)	1.555(3)

Symmetry transformations used to generate equivalent atoms: $^{i}y+1$, $-x+1$, $z+1/4$; ^{ii}x, $y-1$, z; $^{iii}x+1$, y, z; ^{iv}x, $y+1$, z; ^{v}y, $-x+1$, $z+1/4$; $^{vi}x-1$, y, z; $^{vii}-y+1$, x, $z-1/4$; and $^{viii}-y+1$, $x-1$, $z-1/4$.

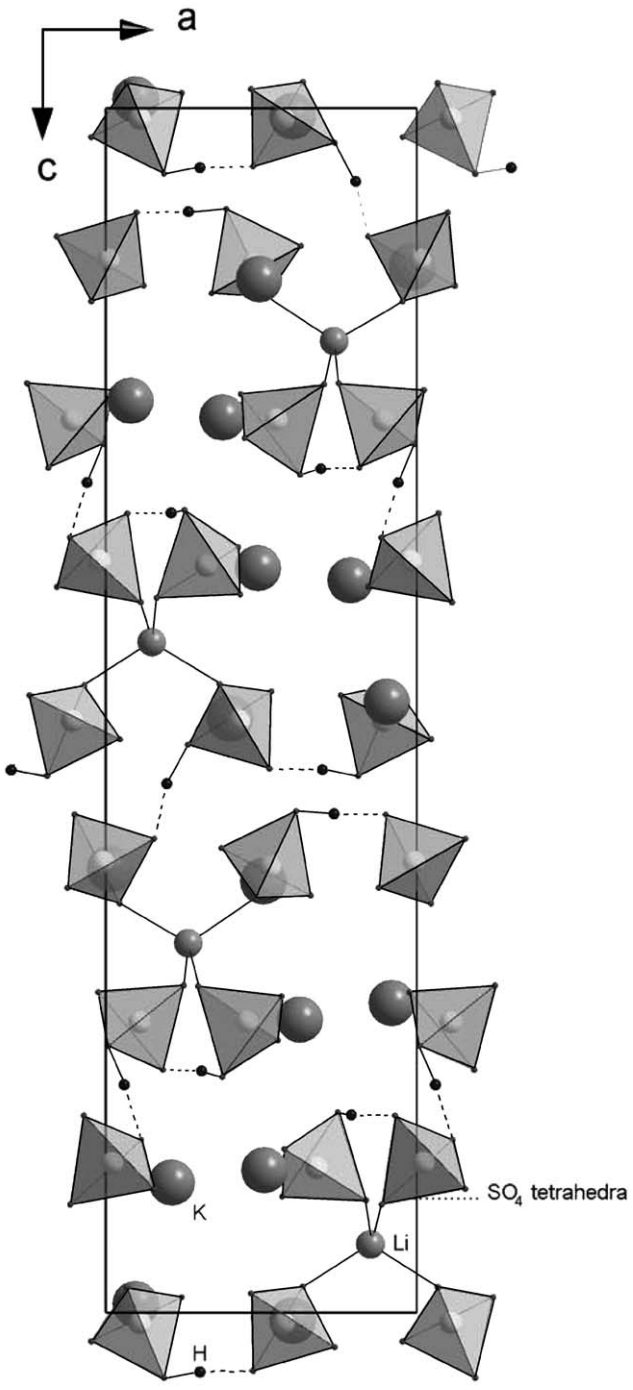

Fig. 3. The unit cell of the KLHS crystal presented along [010].

asymmetric potential well, which was confirmed by the IR spectroscopy measurements [8].

The character of the H1 and H2 bonds remains unchanged with temperature increase. But the differences between donor and acceptor group in the H3 bond decay, d(S2–O23) $\approx$ d(S3-O32), and the position of the proton suggest that this bond became symmetrical at the superionic phase.

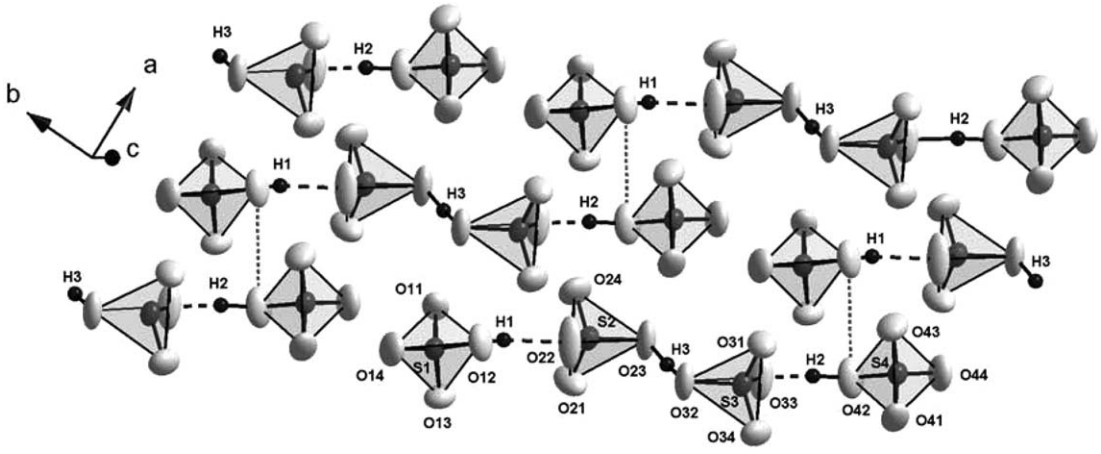

Fig. 4. The SO_4 tetramers arrangement in the double layer (sandwich). The O12–O42 migration paths at the endings of the tetramers are marked by a dotted line.

Table 4
Hydrogen bond parameters for the crystal at 295 and 480 K

Temperature	295 (K)	480 (K)
H1 bond		
O(12)···O(22)^{i}	2.547(3)	2.548(6)
O(12)–H(1)	0.996(64)	0.692(72)
O(22)^{i}···H(1)	1.559(65)	1.864(73)
S1–O(12)	1.547(3)	1.543(4)
S2–O(22)	1.455(2)	1.457(4)
η_d [S(1)–O(12)–H(1)]	112.62(3.11)	113.52(5.74)
η_a [S(2)^{I}–O(22)^{i}–H(1)]	130.02(1.99)	131.07(2.11)
η_H [O(12)–H(1)–O(22)^{i}]	170.38(5.10)	169.54(8.03)
τ [S(1)–O(12)–O(22)^{i}–S(2)^{i}]	10.50	13.05
η'_d [S(1)–O(12)–O(22)^{I}]	117.51(15)	118.31(25)
η'_a [S(2)^{I}–O(22)^{I}–O(12)]	132.76(16)	133.27(25)
H2 bond		
O(42)···O(33)^{ii}	2.532(4)	2.534(6)
O(42)–H(2)	0.960(90)	1.129(80)
O(33)^{ii}···H(2)	1.612(92)	1.418(81)
S4–O(42)	1.555(3)	1.554(4)
S3–O(33)	1.472(3)	1.459(4)
η_d [S(4)–O(42)–H(2)]	115.53(4.84)	114.01(3.78)
η_a [S(3)^{ii}–O(33)^{ii}–H(2)]	130.42(2.89)	126.96(3.03)
η_H [O(42)–H(2)–O(33)^{ii}]	159.14(7.32)	168.27(6.64)
τ [S(4)–O(42)–O(33)^{ii}–S(3)^{ii}]	−14.37	−14.55
η'_d [S(4)–O(42)–O(33)^{ii}]	119.30(15)	120.31(25)
η'_a [S(3)^{i}–O(33)^{ii}–O(42)]	130.73(16)	131.50(25)
H3 bond		
O(23)···O(32)^{iii}	2.500(3)	2.512(5)
O(23)–H(3)	1.116(92)	1.257(66)
O(32)^{iii}···H(3)	1.406(87)	1.270(65)
S2–O(23)	1.530(2)	1.514(4)
S3–O(32)	1.508(2)	1.512(4)
η_d [S(2)–O(23)–H(3)]	119.94(4.73)	118.63(3.15)
η_a [S(3)^{I}–O(32)^{iii}–H(3)]	112.31(3.83)	114.10(3.13)
η_H [O(23)–H(2)–O(32)^{iii}]	164.86(8.40)	167.41(5.87)
τ [S(2)–O(23)–O(32)^{iii}–S(3)^{iii}]	178.42	178.74
η'_d [S(2)–O(23)–O(32)^{iii}]	115.68(13)	116.35(22)
η'_a [S(3)^{iii}–O(32)^{iii}–O(23)]	116.15(14)	116.78(22)

Symmetry transformations used to generate equivalent atoms: ^{i} x, $y-1$, z; ^{ii} $x-1$, y, z; and ^{iii} $y+1$, $-x+1$, $z+1/4$.

3.4. A mechanism of the protonic conductivity

Generally, there are two distinct ways in which protons are transferred through a solid: the vehicular mechanism (where the proton rides on a carrier molecule) or the Grotthuss mechanism (where the proton is transferred between a donor and a suitably situated acceptor molecule) [31]. As was shown, e.g., by Pietraszko et al. [32], Merinov [33], Merinov and Shuvalov [34], Baranov et al. [35], in hydrogen sulfates or selenates of alkali metals crystals (for instance $MeHXO_4$, $Me_3H(XO_4)_2$) the mechanism of a charge transport is of the Grotthuss type, where an XO_4 tetrahedra are the donor and acceptor of protons. An appearance of the superionic phase transition in such crystals is closely related to a libration or even a rotation increase of XO_4 groups with heating, so that the $Me_m(XO_4)_n$ framework loses its rigidity. The phase transformation is accompanied by a group–subgroup crystal symmetry change leading to an excess of structurally equivalent proton sites. As a result, a dynamically disordered hydrogen bonds network is created in a crystal.

A proton transport in a hydrogen bonds network and as a consequence a conductivity activation energy are dependent on: a proton jump along a hydrogen bond from one potential well minimum to the other (most effective for short hydrogen bonds) and an XO_4 groups reorientation, which leads to breaking of an old hydrogen bond and creating a new one (proceeding easily for long hydrogen bonds). Additionally, Merinov and Shuvalov [34] pointed out that H^+ ions relocation is most convenient in gaps or edges between polyhedra that a crystal is composed of.

In the case of the KLHS crystal, the conductivity in [100] and [010] directions is by one order of magnitude higher than in [001]. But even in the [100] or [010]

direction, its value is relatively small (just above T_S, $\sigma \approx 10^{-4}$ S/cm [5,13]) in comparison with other hydrogen sulfates or selenate crystals. Also, an entropy change of this isostructural phase transition is quite small ($\Delta S \approx 0.5$ J/mol K) whereas for instance $\Delta S \approx 9.4$ J/mol K accompanies a superionic phase transition of $Cs_3H(SeO_4)_2$. Nevertheless, a conductivity activation energy lowering from 1.35 to 0.28 eV in [100] allows calling this transition a superionic one.

The two-dimensional character of the proton transport in the KLHS indicates that charge carriers movement through the crystal is closely related to the SO_4 tetrahedra dynamics in sandwiches. The SO_4 tetramer's configuration in double layers creates distances of about 3.25 Å between various oxygen atoms of the SO_4 tetrahedra (except H1, H2, and H3 bonds). These are: O12–O42 between endings of different tetramers (marked by the dotted line in Fig. 4) and O22–O32, O23–O33 (in the middle of the same tetramer). Other distances exceed 3.55 Å. Moreover, a KO_8 and SO_4 polyhedra are arranged in a way that gaps between them occur for the hydrogen bonds and between the endings of the tetramers.

Distances of about 3.25 Å are still too large to form H bond. But an increase in SO_4 tetrahedra librations with temperature increase enables to shorten or to lengthen interatomic distances. The most efficient shortening (in spite of positive thermal expansion parameter) is observed between O12 and O41 where the distance decreases below 2.8 Å. Such a contact is very convenient for the SO_4 tetrahedra reorientation [31]. Simultaneously, the H1, H2 and H3 bond could lengthen up to 3 Å. Breaking of the existing hydrogen bonds in the tetramer and the possible formation of weak, momentary hydrogen bonds, O12–O41, O22–O32 and O23–O33, allow proton to migrate continuously with a mechanism similar to the Grotthuss one. Due to difficulties in finding extra hydrogen positions in long hydrogen bonds by the X-ray diffraction methods, the other H^+ ions transport path could not be excluded but the above-described conductivity mechanism seems to be the most probable one.

4. Summary

The crystal unit-cell parameters measurements and the crystal structure refinement have given us a certainty that the KLHS crystal has tetragonal ($P4_1$) symmetry at room temperature. The crystal retains this symmetry at the investigated temperature range from 8 K to the crystal melting at about 500 K. Therefore, it is difficult to prove the existence of the low-temperature phase transition. On the other hand, if any transition takes place at about 115 K, it is most probably not a ferroelastic transformation.

Similarly, the superionic transition proceeds without symmetry change. But slight changes in the hydrogen bonds network and a significant rise of the SO_4 tetrahedra libration are responsible for the activation energy of conductivity lowering.

The mechanism of the H^+ transport is the Grotthuss type. The H ions are transferred between the donors and the acceptors, breaking and creating momentary hydrogen bonds along the tetramers and between them.

Conductivity temperature dependencies for the rest of the $Me_4LiH_3(XO_4)_4$ crystals, where Me = K, Rb are very similar to each other [5] suggests that the approach proposed for KLHS at the superionic phase transition region may be successfully applied to almost all $MeLHX$ crystals. But a mechanism of the proton transport at $MeLHX$ crystals containing NH_4^+ ions should be described independently. They have a much higher conductivity than the other $MeLHX$ crystals and our results with respect to $(NH_4)_4LiH_3(XO_4)_4$ will be presented in a separate paper.

Acknowledgments

This research was supported by a Grant No. 7 TO8A 027 09 and 2 P03B 170 15 from the Polish Committee for Scientific Research. We would like to thank Professor Z. Gałdecki, Technical University of Łódź, Poland, for giving us the opportunity to use the SHELXTL\PC program and Dr. V.B. Pluzhnikow, Institute of Low Temperature Physics, Ukrainian Academy of Sciences, Kharkov, Ukraine, for the capacitance dilatometry experiment realization.

References

[1] B. Mróz, H. Kiefte, M.J. Clouter, Ferroelectrics 82 (1988) 105.
[2] T. Wołejko, T. Piskunowicz, T. Bręczewski, Krajewski, Ferroelectrics 81 (1988) 175.
[3] H. Hempel, H. Maack, G. Sorge, Phys. Stat. Sol. (a) 110 (1988) 459.
[4] J. Minge, T. Krajewski, Phys. Stat. Sol. (a) 109 (1988) 193.
[5] B. Hilczer, M. Połomska, A. Pawłowski, J. Wolak, Ferroelectrics 155 (1994) 177.
[6] A. Pietraszko, M. Połomska, A. Pawłowski, Izv. A.N. USSR Phys. Ser. 55 (1991) 109.
[7] P. Piskunowicz, T. Breczewski, T. Wołejko, Phys. Stat. Sol. (a) 114 (1989) 505.
[8] S.V. Karpov, T. Krajewski, K.V. Timofeev, Phys. Stat. Sol. (a) 158 (1996) K19.
[9] B. Mroz, R. Laino, Phys. Stat. Sol. (a) 15 (1989) 575.
[10] B. Mróz, H. Kiefte, M.J. Clouter, T.A. Tuszyński, J. Phys.: Condens. Matter 3 (1991) 5673.
[11] F.J. Zuiniga, J. Extebarria, G. Madariaga, T. Br¸eczewski, Acta Crystallogr. C 46 (1990) 1199.
[12] B. Mróz, S.M. Kim, B.M. Powell, H. Kiefte, R.L. Donaberger, Phys. Rev. B 55 (1997) 11174.

[13] M. Połomska, B. Hilczer, J. Wolak, A. Pietraszko, Acta Phis. Polon. A 85 (1994) 825.
[14] G. Brandli, R. Griessen, Cryogenics 13 (1973) 299.
[15] G. Brandli, R. Griessen, R. Pott, R. Schefzyk, J. Phys. E 16 (1983) 444.
[16] W.L. Bond, Acta Crystallogr. 13 (1960) 814.
[17] D. Kucharczyk, A. Pietraszko, K. Łukaszewicz, J. Appl. Crystallogr. 26 (1993) 467.
[18] G.M. Sheldrick, SHELXL-97. Program for the Solution and Refinement of Crystal Structures, University of Göttingen, Germany, 1997.
[19] G.M. Sheldrick, SHELXTL\PC Users Manual, Siemens Analytical X-ray Instruments Inc, Madison, WI, USA, 1990.
[20] M. Połomska, A. Pawłowski, Ferroelectrics 111 (1990) 237.
[21] A. Pietraszko, M. Połomska, A. Pawłowski, Izv. A.N. SSSR. Phys. Ser. 55 (1991) 109.
[22] M. Zimmermann, W. Schranz, J. Phys.: Condens. Matter 8 (1996) 7085.
[23] M. Połomska, A. Pawłowski, Ferroelecrtics 157 (1994) 93.
[24] K. Aizu, J. Phys. Soc. Jpn. 27 (1968) 387.
[25] K. Aizu, Phys. Rev. B 2 (1970) 754.
[26] J. Sapriel, Phys. Rev. B 12 (1975) 5128.
[27] M. Karpinen, J.O. Lundgren, R. Liminga, Acta Crystallogr. C 39 (1983) 34.
[28] A. Katrusiak, Phys. Rev. B 51 (1995) 589.
[29] A. Katrusiak, Phys. Rev. B 48 (1993) 2992.
[30] J.O. Thomas, R. Liminga, Acta Crystallogr. B 34 (1978) 3686.
[31] Ph. Colomban (Ed.), A. Nowak, in: Proton Conductors, Cambridge University Press, Cambridge, 1992.
[32] A. Pietraszko, B. Hilczer, A. Pawłowski, Solid State Ionics 119 (1999) 281.
[33] B.V. Merinov, Solid State Ionics 84 (1996) 89.
[34] B.V. Merinov, L.A. Shuvalov, Kristallografia 37 (1992) 410.
[35] A.I. Baranov, B.V. Merinov, A.V. Tregubchenko, V.B. Khiznichenko, L.A. Shuvalov, N.M. Schagina, Solid State Ionics 36 (1989) 279.